Synthetic, spectral and structural aspects of some mono- and binuclear (homo/hetero) Ru(II) hydrido carbonyl complexes

Manish Chandra [a], Abhaya Nand Sahay [a], Daya Shankar Pandey [a],*,
M. Carmen Puerta [b], Pedro Valerga [b]

[a] *Department of Chemistry, Awadhesh Pratap Singh University, Rewa (M.P.)-486 003, India*
[b] *Departmento de Quimica Inorganica, Universidad de Cadiz, Apartado 40, Puerto Real 11510, Spain*

Abstract

Reactions of the poly-pyridyl bridging ligand 2,4,6-tris(2-pyridyl)-1,3,5-triazine; 2,3-bis(2-pyridyl)-pyrazine and 3,6-bis(2-pyridyl)-1,2,4,5-tetrazine (referred hereafter as tptz, bppz and bptz respectively) with $[RuH(CO)Cl(PPh_3)_3]$ in methanol, gave highly stable cationic complexes with the formulation $[RuH(CO)(PPh_3)_2(L)]^+$. Further, the mononuclear complex $[RuH(CO)(PPh_3)_2(bppz)]PF_6$ reacted with K_2PtCl_4, $[PdCl_2(benzonitrile)_2]$, $[\{Ru(\eta^6-C_{10}H_{14})(\mu-Cl)Cl\}_2]$, $[\{Ru(\eta^6-C_6Me_6)(\mu-Cl)Cl\}_2]$, $[RuCl(\eta^5-C_5H_5)(PPh_3)_2]$ and $[\{Rh(\eta^5-C_5Me_5)(\mu-Cl)Cl\}_2]$ in methanol under refluxing conditions to give bppz bridged binuclear complexes with the formulation $[RuH(CO)(PPh_3)_2(bppz)PtCl_2]PF_6$, $[RuH(CO)(PPh_3)_2(bppz)PdCl_2]PF_6$, $[RuH(CO)(PPh_3)_2(bppz)(\eta^6-C_{10}H_{14})RuCl](PF_6)_2$, $[RuH(CO)(PPh_3)_2(bppz)(\eta^6-C_6Me_6)Cl_2Ru](PF_6)_2$, $[RuH(CO)(PPh_3)_2(bppz)(\eta^5-C_5H_5)(PPh_3)Ru](PF_6)_2$ and $[RuH(CO)(PPh_3)_2(bppz)Rh(\eta^5-C_5Me_5)Cl](PF_6)_2$ in quantitative yield. The reaction products have been characterized by elemental analyses, IR, ^{1}H-, ^{1}H–^{1}H-COSY, ^{13}C-, ^{31}P-NMR, ESMS, FAB mass spectroscopy, electronic spectra and cyclic voltammetry. Molecular structure of the representative mononuclear complex $[RuH(CO)(PPh_3)_2(tptz)]BF_4$ has been confirmed by X-ray crystallography. Crystal structure determination revealed η^2-coordination of the ligand tptz with the metal center. Crystal data: monoclinic, $P2_1/n$, $a = 17.810(6)$ Å, $b = 22.233(9)$ Å, $c = 12.156(4)$ Å, $\beta = 90.06(3)°$, $Z = 4$, $R = 0.078$.
© 2002 Elsevier Science B.V. All rights reserved.

Keywords: Poly-pyridyl ligands; Metallo-ligands; Synthon; Supramolecules

1. Introduction

Synthesis and characterization of ruthenium complexes containing poly-pyridyl bridging ligands have received considerable recent attention, owing to their interesting photophysical and photochemical properties, their possible use in photochemical molecular devices and as light sensitive probes in biological systems [1a–g]. The polyazine ligands in general, have energetically low lying π* orbitals, which can accept a lone pair of electrons from filled metal d orbitals of π symmetry. As a consequence, they exhibit reversible reduction processes and very intense solvatochromic charge transfer bands in the visible region. In addition, properly tuned metal ligand charge transfer excited states play a very significant role in the photosubstitution and intramolecular energy transfer reactions [2a–c]. In this regard, bridging ligands viz. 2,3-bis(2-pyridyl)-pyrazine (bppz), 3,6-bis(2-pyridyl)-1,2,4,5-tetrazine (bptz), 2,4,6-tris(2-pyridyl)-1,3,5-triazine (tptz) and other related diimines have drawn special attention and have extensively been used in the synthesis of mono- and polynuclear, homo- and heterometallic complexes possessing interesting spectroscopic, photophysical and photochemical properties [3a–g].

Because of current interests in the poly-pyridyl ligands and in continuation of our studies towards synthesis of *metallo-ligands/synthons* based on organometallic systems, which could be employed in the synthesis of homo/hetero bi- or polynuclear complexes [4], we have made a detailed study on reactivity of the poly-pyridyl bridging ligands viz. 2,3-bis(2-pyridyl)-pyrazine, 3,6-bis(2-pyridyl)-1,2,4,5-tetrazine, 2,4,6-tris(2-pyridyl)-

* Corresponding author. Tel.: + 91-766-240-740.
E-mail addresses: dsprewa@yahoo.com (D.S. Pandey), carmen.puerta@uca.es (M.C. Puerta).

1,3,5-triazine with the ruthenium(II) complex [RuH-(CO)Cl(PPh$_3$)$_3$]. We found that such a reaction led in the formation of mononuclear complexes with the general formulation [RuH(CO)(PPh$_3$)$_2$(L)]$^+$ Further, to evaluate applicability of the mononuclear complexes as building blocks in the synthesis of homo/hetero binuclear complexes, we have reacted the representative complex [RuH(CO)(PPh$_3$)$_2$(bppz)]PF$_6$, with different molecules ranging from K$_2$PtCl$_4$, [PdCl$_2$(benzonitrile)$_2$], chloro-bridged dimeric arene ruthenium complexes [{Ru(η^6-arene)(μ-Cl)Cl}$_2$] (arene = *p*-cymene or hexamethylbenzene), [RuCl(η^5-C$_5$H$_5$)(PPh$_3$)$_2$] and [{Rh(η^5-C$_5$Me$_5$)(μ-Cl)Cl}$_2$]. We found that the mononuclear complex [RuH(CO)(PPh$_3$)$_2$(bppz)]PF$_6$ behaves as a potential metallo-ligand and led in the formation of binuclear complexes. In this paper we report reproducible syntheses and spectral characterization of mononuclear complexes [RuH(CO)(PPh$_3$)$_2$(L)]$^+$ (L = tptz, bppz or and bptz) and homo and hetero binuclear bppz bridged complexes [RuH(CO)(PPh$_3$)$_2$(bppz)PtCl$_2$]PF$_6$, [RuH-(CO)(PPh$_3$)$_2$(bppz)PdCl$_2$]PF$_6$, [RuH(CO)(PPh$_3$)$_2$(bppz)-(η^6-C$_{10}$H$_{14}$)RuCl](PF$_6$)$_2$, [RuH(CO)(PPh$_3$)$_2$(bppz)(η^6-C$_6$Me$_6$)RuCl](PF$_6$)$_2$, [RuH(CO)(PPh$_3$)$_2$(bppz)(η^5-C$_5$-H$_5$)(PPh$_3$)Ru](PF$_6$)$_2$, and [RuH(CO)(PPh$_3$)$_2$(bppz)Rh-(η^5-C$_5$Me$_5$)Cl](PF$_6$)$_2$. Also, we present herein, single crystal X-ray structure of the representative mononuclear complex [RuH(CO)(PPh$_3$)$_2$(tptz)]BF$_4$.

2. Results and discussion

The cationic mononuclear complexes with the general formulation [RuH(CO)(PPh$_3$)$_2$(L)]$^+$ (L = tptz, bptz or bppz) could easily be prepared in quantitative yield by reaction of [RuH(CO)Cl(PPh$_3$)$_3$] with the bridging ligands in methanol in 1:1 molar ratio.

Where L = tptz, bppz, bptz
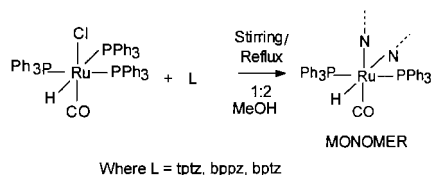
The mononuclear complexes [RuH(CO)(PPh$_3$)$_2$-(tptz)]BF$_4$ (**1**), [RuH(CO)(PPh$_3$)$_2$(bppz)]BF$_4$ (**2**), [RuH-(CO)(PPh$_3$)$_2$(bppz)]PF$_6$ (**3**) and [RuH(CO)(PPh$_3$)$_2$-(bptz)]PF$_6$ (**4**) are bright yellow to golden orange, airstable, non-hygroscopic shiny crystalline solids. These are sparingly soluble in dichloromethane, chloroform, methanol and ethanol, highly soluble in acetone, acetonitrile, dimethylsulfoxide, and dimethylformamide, and insoluble in benzene, petroleum ether, and diethyl ether. These exhibit 1:1 conductance behavior in nitromethane. Our preliminary studies on reactivity of the complexes [RuH(CO)(PPh$_3$)$_2$(L)]$^+$ indicated that these

systems behave as potential *metallo-ligands*, which could be employed as building blocks in the synthesis of supramolecular systems. Reaction of complex **3** with K$_2$PtCl$_4$, [PdCl$_2$(benzonitrile)$_2$], [{Ru(η^6-C$_{10}$H$_{14}$)(μ-Cl)-Cl}$_2$], [{Ru(η^6-C$_6$Me$_6$)(μ-Cl)Cl}$_2$], [RuCl(η^5-C$_5$H$_5$)-(PPh$_3$)$_2$] and [{Rh(η^5-C$_5$Me$_5$)(μ-Cl)Cl}$_2$], in methanol under refluxing conditions gave binuclear complexes [RuH(CO)(PPh$_3$)$_2$(bppz)PtCl$_2$]PF$_6$ (**5**), [RuH(CO)-(PPh$_3$)$_2$(bppz)PdCl$_2$]PF$_6$ (**6**), [RuH(CO)(PPh$_3$)$_2$(bppz)-(η^6-C$_{10}$H$_{14}$)RuCl](PF$_6$)$_2$ (**7**), [RuH(CO)(PPh$_3$)$_2$(bppz)-(η^6-C$_6$Me$_6$)RuCl](PF$_6$)$_2$ (**8**), [RuH(CO)(PPh$_3$)$_2$-(bppz)(η^5-C$_5$H$_5$)(PPh$_3$)Ru](PF$_6$)$_2$ (**9**) and [RuH(CO)(PPh$_3$)$_2$-(bppz)Rh(η^5-C$_5$Me$_5$)Cl](PF$_6$)$_2$ (**10**) in quantitative yield.

Carbon, hydrogen and nitrogen analyses of all the complexes conformed well to their formulations. Further information about composition of the complexes has also been obtained from ESMS, which is one of the recent techniques being used as a powerful tool for characterization of the complex systems [5a,b] and FAB mass spectrometry (FABMS), ESMS spectra of complexes **1** and **2** showed prominent peaks at *m/z* 967.2 (100%) and 891 (100%), respectively, corresponding to [RuH(CO)(PPh$_3$)$_2$(tptz)]$^+$ and [RuH(CO)(PPh$_3$)$_2$-(bppz)]$^+$, which is consistent with our formulations. In the FABMS of complex **1** the molecular ion peak corresponding to [RuH(CO)(η^2-tptz)(PPh$_3$)$_2$]$^+$ appeared at *m/z* 967 (calc. 967). Presence of the peaks at *m/z* 704 (calc. 704), *m/z* 675 (calc. 675), *m/z* 414 (calc. 413) corresponding to [RuH(CO)(η^2-tptz)(PPh$_3$)]$^+$, [Ru(η^2-tptz)(PPh$_3$)]$^{2+}$ and [Ru(η^2-tptz)]$^{2+}$ moieties in the FABMS of the complex **1** further supported formulation of the complex.

FABMS of the complexes **5**, **7**, **8** and **10** displayed prominent peaks at *m/z* 889 (calc. 889); 1309 (calc. 1306); 1160 (calc. 1157); 1333 (calc. 1333) and 1155 (calc. 1154), respectively, corresponding to the cationic species [RuH(CO)(PPh$_3$)$_2$(bppz)PtCl$_2$]$^+$, {[RuH(CO)-(PPh$_3$)$_2$(bppz)(η^6-C$_{10}$H$_{14}$)RuCl](PF$_6$)}$^+$, {[RuH(CO)-(PPh$_3$)$_2$(bppz)(η^6-C$_6$Me$_6$)RuCl](PF$_6$)}$^+$ and {[RuH-(CO)(PPh$_3$)$_2$(bppz)Rh(η^5-C$_5$Me$_5$)](PF$_6$)}$^+$. Presence of these peaks in the FAB mass spectra of the respective complexes and overall fragmentation patterns are consistent with the formulation of the binuclear complexes.

Infrared spectra of the complexes exhibited characteristic bands due to coordinated ligands tptz, bppz, bptz, PPh$_3$, CO and hydride group in the respective complexes. Interestingly, the position of v(C≡O) and v(Ru–H) in the IR spectra of the complexes shifted toward higher and lower frequency. It indicated a decrease in the metal to carbonyl carbon interaction and an increase in the Ru–H bond order.

The ^{1}H-NMR spectra of the complexes have been assigned using the atom numbering scheme shown in Fig. 1. ^{1}H-NMR data of all these complexes are given in Section 3. To facilitate assignment of the resonances,

^1H–^{1}H-COSY experiment was carried out and the resulting spectrum of complex **1** is shown in Fig. 2. The doublets are assigned to the protons at 3 and 6 positions and triplets to the protons at 4 and 5 positions. The ^{1}H-NMR spectra of the complex **1** exhibited distinct signals at δ 8.92 (d, 1H, 4.2 Hz), 8.60 (d, 1H, 7.8 Hz), 8.14 (t, 3H, 6.6 Hz), 7.92 (t, 1H, 6.6 Hz), 7.72 (t, 1H, 7.2 Hz), and 7.52 (br s, 1H) along with a broad multiplet due to aromatic protons of PPh$_3$ in the region δ 7.27–7.33 ppm and a triplet in the high field side at −11.3 ppm. The lowest field doublet at δ 8.92 ppm with J_{H-H} value of 4.2 Hz have been assigned to H_6' and the doublet at δ 8.60 ppm with J_{H-H} value of 7.8 Hz

have been assigned to H$_3$ proton by comparison of J_{H-H} values in free tptz ligand. The resonance at δ 8.14, 7.92, and 7.72 ppm have been assigned to $H_5' + H_4$, H_4' and H_5 protons, respectively. The broad singlet at δ 7.52 ppm has been assigned to H$_6$ proton. Upfield shift of this signal could be attributed to the shielding of this proton from π back-bonding ability of Ru(II) which increases electron density on metal bound nitrogen and on adjacent atoms [3f]. In the ^{1}H-NMR spectra of complex **2**, distinct resonances are displayed at δ 9.15, 8.62, 8.16 and 6.62 ppm and overlapping resonance in the region 7.91–7.18 ppm. In its ^{1}H-NMR spectra, doublets are expected for the protons at 3, 6 and 3′, 6′

Fig. 1. Numbering of protons in the complex cations of **1**, **3** and **4**.

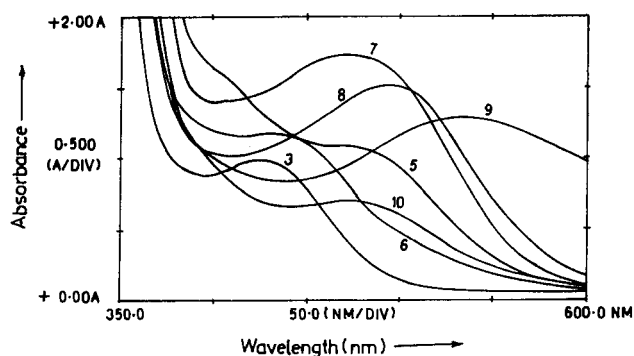Fig. 2. ^{1}H–^{1}H-COSY spectrum of complex **1**.

Fig. 3. Electronic spectra of the binuclear complexes 3, 5–10 in acetone.

position, triplets are expected for the protons at 4, 5 and 4′, 5′ positions, while the protons 1 and 2 are expected to show one signal each and split as doublets. Interestingly, the protons 1 and 2 appeared as doublets at δ 7.77 and 7.63 ppm. The doublets at δ 9.16 and 8.16 have been assigned to H_3 and H_6 protons overlapping resonance in the region 7.91–7.31 ppm could not be precisely assigned, since this region is highly crowded by aromatic protons of PPh_3 ligand. The doublet at δ 6.62 ppm has been assigned H_6' proton. It showed an upfield shift and is consistent with the shielding of protons adjacent to metal bound nitrogen [6a–b].

In the ^{1}H-NMR spectra of complex 4, the doublets at δ 8.92, 8.78, and 8.74 and 8.70 ppm have been assigned to $H_6 + H_6'$ and $H_3 + H_3'$ protons, while the triplets at δ 8.11, 8.20, 7.95 and 7.02 ppm have been assigned to H_5, H_5' and H_4, H_4' protons. Aromatic protons of PPh_3 ligand resonated as a broad multiplet in the region δ 7.52–7.18 ppm.

An interesting feature of the ^{1}H-NMR spectra of the complexes 1, 2 and 3 are the hydrido resonance in the high field side at δ −11.93 ($J_{P–H} = 29.4$ Hz), −11.7 ($J_{P–H} = 30.1$ Hz) and −12.18 ppm (26.7 Hz), respectively. The presence of a triplet corresponding to the metal bound hydride proton in the ^{1}H-NMR spectra of these complexes suggested that the hydride group be coupled with two equivalent ^{31}P nuclei [7].

The ^{31}P{^{1}H}-NMR spectra of these complexes 1, 2 and 3 displayed sharp singlets at δ 46.54, 50.95 and 48.6 ppm, respectively. It indicated that both the triphenylphosphine ligands in these complexes are equivalent and are mutually *trans* disposed.

2.1. Electronic spectra

Electronic spectra of the complexes follow typical trends observed in ruthenium polyazine complexes, which display ligand based $\pi \rightarrow \pi^*$ transitions for each polyazine ligand in the ultra-violet region and metal to ligand charge transfer MLCT transitions for each acceptor ligand in the visible region. Interaction of the

filled orbitals of proper symmetry on d^6 Ru(II), with the low lying π^* orbital of the ligands tptz, bppz or bptz should provide MLCT transition ($t_{2g} \rightarrow \pi^*$) in the electronic spectra of these complexes, with the transition energy varying with nature of the ligands acting as a π acceptor. In the electronic spectra of complex 1, three strong absorption were observed at about 441, 389, and 335 nm. On the basis of the intensity and position of the lowest energy absorption, it has been assigned to MLCT transition [8], while the one at $\sim$389 nm may be of MLCT character, but the possibility of σ bond to ligand charge transfer SBLCT cannot be ruled out [9]. The high-energy band has been assigned to intra-ligand $\pi \rightarrow \pi^*$ transition or π (phenyl) to π^* (phenyl) transition [10]. Electronic spectra of the bimetallic complexes in acetonitrile at room temperature are shown in Fig. 3. These displayed intense peaks throughout the ultra-violet and visible region of the spectrum. The mononuclear ruthenium complex 3, [RuH(CO)(PPh$_3$)$_2$(bppz)]PF$_6$, from which the binuclear complexes have been prepared, displayed bands at 426, 336 and 298 nm. The low energy band at 426 nm has been assigned to Ru $\rightarrow$ bppz CT transition, while the one at 336 nm has been assigned to intra-ligand $\pi \rightarrow \pi^*$ transition. It was further observed that Ru $\rightarrow$ bppz CT transition of complex 3, upon interaction with another metal center through bridge formation on the bppz ligand, exhibited significant red shifts [complex 5, 480; 6, 472; 7, 475; 8, 493; 9, 544 and 10, 465 nm] as compared to that in the mononuclear complex 3. The red shift in the position of Ru $\rightarrow$ bppz CT transition towards lower energy in these complexes may result from stabilization of bppz π^* orbital upon coordination of the second metal center. In general, the coordination of another metal ion at the remote coordination site results in stabilization of the π^* level of the bridging ligand leading to enhanced π–π^* overlap [11]. This effect lowers the HOMO–LUMO gap, which results in a lower energy shift of the MLCT bands in the binuclear complexes. The stabilization of the bppz π^* also leads to a red shift of the ligand based $\pi \rightarrow \pi^*$ transitions. These observations strongly support the formation of the binuclear complexes and are consistent with other reports [3f].

2.2. Electrochemistry

The cyclic voltammograms for the mononuclear complexes 1, 2 and 4 are shown in Fig. 4. The plots of the peak currents versus square root of the scan rates are linear for all the complexes, indicating that diffusion controlled processes occur at the electrodes. On the cathodic side of the CV scan all the complexes exhibit one or more ligand centered reductions, localized over polyimine ligands. These are invariably observed at more negative potentials than the former. The

analogous poly-pyridyl centered reductions in $[(bipy)_2Ru(poly-py)]^{2+}$ are observed between -1.0 and -1.5 V versus Ag/AgCl under similar conditions [12a–c]. The ligand centered reduction in the complexes **1**, **2** and **4** are observed at -0.73, -0.61 and -0.66 V versus Ag | AgCl in acetonitrile, respectively [3f]. It therefore indicates that the M–L σ bond is stronger in these complexes.

On the anodic side of the CV scan, these complexes exhibit two consecutive oxidation waves. Analogous phosphine complexes $[Ru(PPh_3)_2(CO)Cl]$ are known to catalyze electro-oxidation of CO to CO_2 in solution [13]. The second oxidation wave at 1.1 V versus Ag | AgCl is expected to arise due to electron transfer from coordinated CO. The first oxidation at 0.48 V
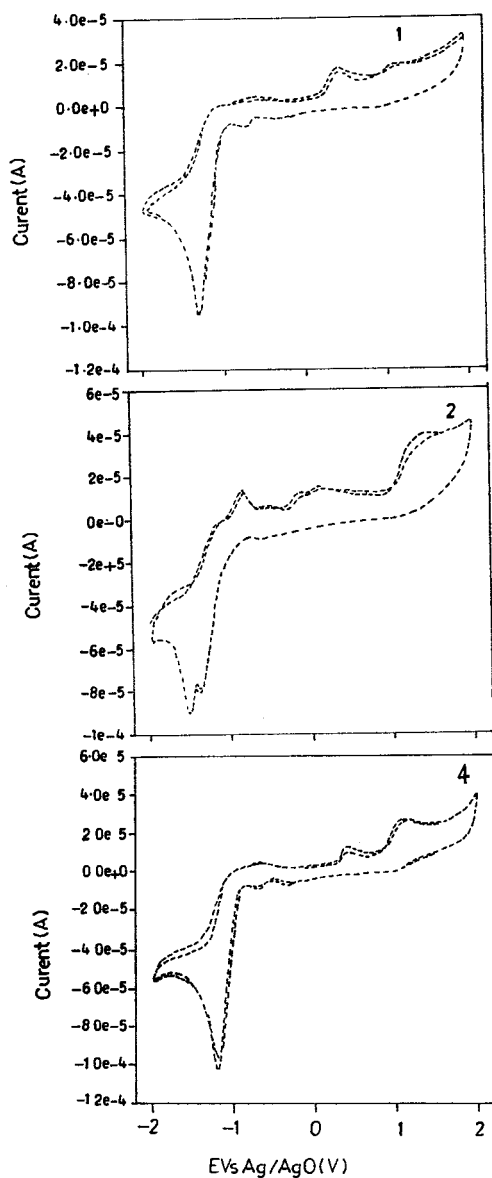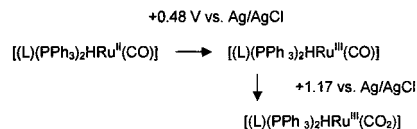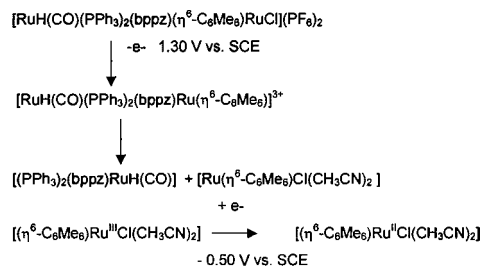

Fig. 4. Cyclic voltammograms of the complexes **1**, **2** and **4** in acetonitrile.

versus Ag | AgCl arises from oxidation of the metal center [i.e. Ru(II) → Ru(III) processes]. Thus the oxidation can be described as below.

$$+0.48 \text{ V vs. Ag/AgCl}$$
$$[(L)(PPh_3)_2HRu^{II}(CO)] \longrightarrow [(L)(PPh_3)_2HRu^{III}(CO)]$$
$$\downarrow \quad +1.17 \text{ vs. Ag/AgCl}$$
$$[(L)(PPh_3)_2HRu^{III}(CO_2)]$$

The binuclear complex **8** exhibits a quasi-reversible oxidation wave at Ep $+1.30$ V and an irreversible reduction wave at -0.80 V versus SCE in acetonitrile. These waves seem to arise from $[(C_6Me_6)Ru(II/III)]$ and electron transfer to the coordinated bppz moieties, respectively. However, if the cathodic scan is preceded by the anodic scan, an additional irreversible reduction wave appears at Ep -0.50 V versus SCE. It seems that $(\eta^6-C_6Me_6)RuCl$ moiety in complex **8** undergoes a metal centered oxidation followed by the dissociation of the oxidized fragment. This solvated-oxidized fragment is subsequently undergoing reduction at Ep -0.50 V.

$$[RuH(CO)(PPh_3)_2(bppz)(\eta^6-C_6Me_6)RuCl](PF_6)_2$$
$$\downarrow \text{ -e- } 1.30 \text{ V vs. SCE}$$
$$[RuH(CO)(PPh_3)_2(bppz)Ru(\eta^6-C_6Me_6)]^{3+}$$
$$\downarrow$$
$$[(PPh_3)_2(bppz)RuH(CO)] + [Ru(\eta^6-C_6Me_6)Cl(CH_3CN)_2]$$
$$+ \text{ e-}$$
$$[(\eta^6-C_6Me_6)Ru^{III}Cl(CH_3CN)_2] \longrightarrow [(\eta^6-C_6Me_6)Ru^{II}Cl(CH_3CN)_2]$$
$$- 0.50 \text{ V vs. SCE}$$

However, if the anodic scan is taken with the switching potential (E_λ) -1.50 V versus SCE, an additional reversible reduction wave is observed at $E_{1/2}$ -1.07 V versus SCE. This wave seems to arise from the Ru(II)/Ru(III) process centered at $[(PPh_3)_2RuH(bppz)]$ moiety.

2.3. Single crystal X-ray structure of the complex $[RuH(CO)(PPh_3)_2(tptz)]BF_4$

Structure of complex **1** has been confirmed by single crystal X-ray diffraction analysis. An ORTEP view of the complex cation along with the atom numbering is shown in Fig. 5. Selected bond angles and bond lengths are recorded in Tables 2 and 3, respectively. Geometry about the Ru(II) center is distorted octahedron formed by N(1) and N(4) from the ligand tptz, P(1) and P(2) from the triphenylphosphine ligands, carbonyl carbon C(1) and the hydride ligand H(1). The nitrogen atoms N(1), N(4), C(1) and H(1) form the equatorial base and the phosphine ligands are in axial position. The triazine ring and coordinated pyridyl ring are co-planar and the Ru(II) ion is contained in the least squares plane through the atoms N(1), C(2), N(3), C(3), N(2), C(4), C(5), C(6), C(7), C(8), C(9), and N(4) (mean deviation 0.0581 Å). The uncoordinated pyridyl groups are out of
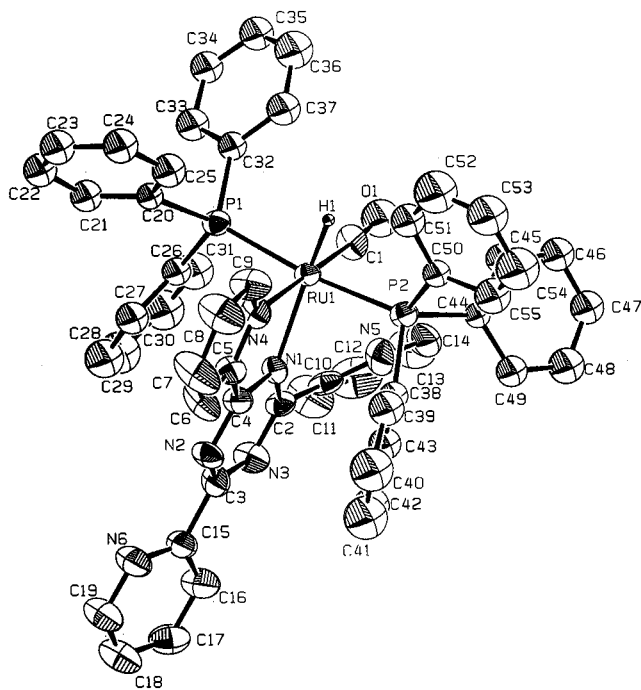
Fig. 5. ORTEP view of the complex cation of **1** (hydrogen atoms and BF$_4$ anion has been removed for clarity).

Table 1
Summary of crystal data and crystal structure analysis for complex **1**

Empirical formula	C$_{55}$H$_{43}$BF$_4$N$_6$OP$_2$Ru
Formula weight	1053.81
Color, shape	Orange, plate
Crystal size (mm)	$0.35 \times 0.25 \times 0.10$
Crystal system	Monoclinic
Space group	$P2_1/n$
a (Å)	17.810(6)
b (Å)	22.233(9)
c (Å)	12.156(4
β (°)	90.06(3)
V (Å^3)	4813(2)
Z	4
D_{calc} (g cm^{-3})	1.454
μ(Mo–K$_\alpha$) (cm^{-1})	4.45
$F(000)$	2152.00
Unique reflections	7181($R_{int} = 0.1082$)
Observed reflections ($I > 3\sigma$)	3626
Number of parameters	421
R [a]	0.0784
R_w (w = σ_F^{-2}) [b]	0.0916
Goodness-of-fit	2.312
Max/min residuals (e Å^{-3})	+1.26, −1.16

[a] $R = \Sigma(F_o - F_c)/\Sigma F_o$.
[b] $R_w = [\Sigma w(F_o^2 - F_c^2)^2/\Sigma(F_o^2)]^{1/2}$.

the above plane. The N(1)–Ru(1)–N(4) angle of 76.1(4)° suggested inward bending of the coordinated pyridyl group. The smaller value of N(1)–Ru(1)–N(4) bite angle 76.1(4)° as compared to the ideal value of 90° is probably the source of observed distortion. The Ru(1) to central triazine N(1) bond length is 2.25(1) Å

and it is slightly larger than the Ru(II) to coordinated pyridyl nitrogen N(4) [2.168(10) Å]. These are comparable to those reported for Ru(II) poly pyridyl complexes. The triphenylphosphine ligands lie in *trans* position as indicated by the P(1)–Ru(1)–P(2) angle of 173.4(1)°. The Ru(1)–P(1) and Ru(1)–P(2) distances are 2.347(4) and 2.385(4) Å, respectively. These are essentially equivalent and comparable to those in other related complexes [14]. The Ru(1)–C(1) bond length is 1.81(1) Å, which is normal for Ru(II) carbonyls [15a,b]. The Ru(1)–H(1) distance in the complex cation is 1.458 Å. It is slightly shorter than those found in [RuH(H$_2$O)(CO)$_2$(PPh$_3$)$_2$]$^+$ (1.7 Å), [RuHCl(PPh$_3$)$_3$] (1.7 Å), and other related systems [16a–c].

The average C–C bond length within the ring is 1.375(2) Å, while, the average intra-ring C–N bond length is 1.34(2) Å. These values are comparable with average C–C bond distances of 1.39 Å and C–N bond distances of 1.34 Å.

It is well established that the ligand tptz is susceptible for metal-promoted hydrolysis and gives 2-pyridylcarbonylamide anion (bpca) and 2-picolinamide [17]. In this regard, complex **1** is highly stable, even after refluxing for 48 h in ethanol–water (1:1), it did not show any metal promoted hydrolysis. At the same time, metal induced hydroxylation at the carbon atom of the triazine ring has also not been observed with complex **1**. The present study clearly revealed that the mononuclear complex [RuH(CO)(PPh$_3$)$_2$(bppz)]PF$_6$ acts as a *synthon* and offers a unique opportunity of behaving as a potential *metallo-ligand* in the synthesis of homo/hetero binuclear complexes. The analytical, NMR, FABMS, electronic spectral and electrochemical data of complexes **5–10** provide strong evidence in favor of formation of binuclear complexes starting from complex [RuH(CO)(PPh$_3$)$_2$(bppz)]PF$_6$. However, at this

Table 2
Selected bond angles (°) for complex **1** (estimated S.D.s are given in parentheses)

P(1)–Ru(1)–P(2)	173.4(1)	P(1)–Ru(1)–N(1)	93.4(3)
P(1)–Ru(1)–N(4)	95.3(3)	P(1)–Ru(1)–C(1)	85.8(5)
P(1)–Ru(1)–H(1)	94.4151	P(2)–Ru(1)–N(1)	93.2(3)
P(2)–Ru(1)–N(4)	86.7(3)	P(2)–Ru(1)–C(1)	92.2(5)
P(2)–Ru(1)–H(1)	79.2516	N(1)–Ru(1)–N(4)	76.1(4)
N(1)–Ru(1)–C(1)	104.5(6)	N(1)–Ru(1)–H(1)	165.4153
N(4)–Ru(1)–C(1)	178.7(6)	N(4)–Ru(1)–H(1)	90.9514
C(1)–Ru(1)–H(1)	88.3770		

Table 3
Selected bond lengths (Å) for the complex **1** (estimated S.D.s are given in parentheses)

Ru(1)–P(1)	2.347(4)	Ru(1)–P(2)	2.385(4)
Ru(1)–N(1)	2.25(1)	Ru(1)–N(4)	2.1688(10)
Ru(1)–C(1)	1.81(1)	Ru(1)–H(1)	1.4582

stage it has not been possible for us to confirm the structure of any of the binuclear complexes by single crystal X-ray diffraction studies. More detailed work in this direction is in progress in our laboratory.

3. Experimental

All the reactions were carried out under nitrogen atmosphere and with deaerated solvents. The solvents were of AR grade and were purified by standard procedures prior to their use. Electrochemical data of the complexes were obtained in MeCN which was pre-passed through activated neutral alumina (previously dried at 110 °C for 24 h). 2,3-Bis(2-pyridyl)-pyrazine, 3,6-bis(2-pyridyl)-1,2,4,5-tetrazine, 2,4,6-tris(2-pyridyl)-1,3,5-triazine, ammonium tetrafluoroborate, ammonium hexafluorophosphate, ruthenium(III) chloride hydrate (all Aldrich) and tetrabutylammonium perchlorate (Fluka) were used as received without further purification. The precursor complex [RuH(CO)Cl-(PPh$_3$)$_3$] was prepared and purified following the literature procedure [18].

3.1. Physical measurements

Microanalyses were performed by the micro-analytical section of the Regional Sophisticated Instrumentation Centre, Central Drug Research Institute, Lucknow. Conductivity measurements were made on a Systronics-306 conductivity bridge. Infrared spectra and electronic spectra were recorded on Shimadzu-8201PC and Shimadzu-UV-160 spectrophotometers, respectively. ^{1}H-, ^{1}H–^{1}H-COSY, ^{13}C- and ^{31}P-NMR spectra were recorded on a Bruker DRX-300 NMR instrument. The ESMS were recorded on a Micromass-Quattro-II triple quadrupole mass spectrometer. The samples were introduced into the ESI source through a syringe pump at 0.4 ml h^{-1}. The ESI capillary was 3.5 kV and cone-voltage 25–50 V. The spectra were collected in 4 s scans and print outs are averaged spectra of 5–10 scans. FAB mass spectra were recorded on a JEOL SX 102/DA 6000 mass spectrometer using Xenon (6 kV, 10 mA) as the FAB gas. The accelerating voltage was 10 kV and the spectra were recorded at room temperature (r.t.) with m-nitrobenzyl alcohol as the matrix. The cyclic voltammograms were recorded on a Solartron-1287 electrochemical system in deaerated MeCN in presence of 0.1 M tetrabutylammonium perchlorate as supporting electrolyte using three electrode assembly at different scan rates, with Pt working electrode, Pt wire counter electrode and Ag | AgCl reference electrodes.

3.2. Preparation of the complexes

3.2.1. Preparation of [RuH(CO)(PPh$_3$)$_2$(tptz)]BF$_4$ (**1**)

A suspension of [RuH(CO)Cl(PPh$_3$)$_3$] (955 mg, 1 mmol) in MeOH (60 ml) was treated with tptz (312 mg, 1 mmol) and the resulting solution was heated under reflux for ∼20 h. The precursor complex [RuH(CO)Cl(PPh$_3$)$_3$] slowly dissolved and gave a bright orange–red solution. It was cooled to r.t. and filtered through celite to remove any solid residue. Saturated solution of NH$_4$BF$_4$ in methanol (25 ml) was added to the filtrate, rotaporated to about 25 ml, and was left in a refrigerator for slow crystallization. Crystalline product appeared in a couple of days quantitatively. The crystals were separated by filtration, washed with MeOH, Et$_2$O, and dried in vacuo. Yield: 80% (868 mg); Anal. Found: C, 62.95; H, 4.13; N, 7.60. Calc. for C$_{55}$H$_{43}$BF$_4$N$_6$OP$_2$Ru: C, 62.67; H, 4.08; N, 7.97%. ESMS (m/z): 967.2 Calc. for [RuH(CO)(PPh$_3$)$_2$(tptz)]$^+$ (968). FABMS m/z obs. (calc.): 967 (967), 704 (704), 675 (675), 414 (413); IR (cm^{-1}, nujol): 2005 ν(Ru–H), 1955 ν(CO), 1635, 1575, 1537, 1500, 1433, 1363, 1311, 1155, 1033, 995, 848, 746, 696 (bands due to tptz, PPh$_3$, and counter anion BF$_4^-$); ^{1}H-NMR (δ ppm, acetone-d_6, 300 MHz, 25 °C): 8.92 (d, 1H, 4.2 Hz), 8.60 (d, 1H, 7.8 Hz), 8.14 (t, 3H, 6.6 Hz), 7.92 (t, 1H, 6.6 Hz), 7.72 (t, 1H, 7.2 Hz), 7.52 (s, 1H), −11.93 (t, 1H, 29.4 Hz); ^{31}P{^{1}H}: 46.54 (s); UV–vis (λ_{max} nm): 441, 389, 335.

3.2.2. Preparation of [RuH(CO)(PPh$_3$)$_2$(bppz)]BF$_4$ (**2**)

Complex **2** was prepared by the same method as described for complex **1** starting from [RuH(CO)Cl-(PPh$_3$)$_3$] (477 mg, 0.5 mmol) and bppz (117 mg, 0.5 mmol). The complex separated as bright yellow needles. Yield: 75% (366 mg, 0.75 mmol); Anal. Found: C, 63.16; H, 4.23; N, 5.34. Calc. for C$_{51}$H$_{41}$BF$_4$N$_4$OP$_2$Ru: C, 62.76; H, 4.20; N, 5.74%. ESMS (m/z): 889.1 (Calc. for [RuH(CO)(PPh$_3$)$_2$(bppz)]$^+$ (889); IR (cm^{-1}, nujol): 2003 ν(Ru–H), 1960 ν(CO), 1590, 1572, 1555, 1548, 1520, 1445, 1365, 1315, 1252, 1160, 1030, 986, 840, 735, 690, (bands due to bppz, PPh$_3$ and counter anion BF$_4^-$); ^{1}H-NMR (δ ppm, acetone-d_6, 300 MHz, 25 °C): 9.15 (d), 8.62 (d), 8.16 (m), 8.12–7.8 (m), 7.62–7.59 (m), 7.42–6.96 (br, m), −11.3 (t); ^{31}P{^{1}H} δ 50.95 ppm (s); UV–vis (λ_{max} nm): 426, 336, 298.

3.2.3. Preparation of [RuH(CO)(PPh$_3$)$_2$(bppz)]PF$_6$ (**3**)

Complex **3** was prepared by the same method as described for complex **2** starting from [RuH(CO)Cl-(PPh$_3$)$_3$] (477 mg, 0.5 mmol) and bppz (117 mg, 0.5 mmol). It separated as bright yellow needles. Yield: 75% (366 mg, 0.75 mmol); Anal. Found: C, 58.69; H, 4.21; N, 5.25. Calc. for C$_{51}$H$_{41}$F$_6$N$_4$OP$_3$Ru: C, 59.24; H, 3.96; N, 5.42%. FABMS (m/z): 889.1 (Calc. for [RuH(CO)(PPh$_3$)$_2$(bppz)]$^+$ (889); UV–vis (λ_{max} nm): 426, 336, 298.

3.2.4. Preparation of [RuH(CO)(PPh₃)₂(bptz)]PF₆ (4)

3.2.4. Preparation of [RuH(CO)(PPh$_3$)$_2$(bptz)]PF$_6$ (4)

Complex **4** was prepared following the above procedure starting from [RuH(CO)Cl(PPh$_3$)$_3$] (477 mg, 0.5 mmol) and bptz (118 mg, 0.5 mmol). Red–brown crystals separated out. Yield of the complex was found to be very poor, $\sim 40\%$ (390 mg, 0.4 mmol). Anal. Found: C, 56.7; H, 3.76; N, 7.35. Calc. for C$_{49}$H$_{39}$F$_6$N$_6$OP$_3$Ru: C, 56.7; H, 3.96; N, 8.10%. IR (cm^{-1}, nujol): 2000 ν(Ru–H), 1949 ν(CO), 1627, 1575, 1539, 1502, 1477, 1433, 1359, 1311, 1255, 1184, 1159, 1091, 840, 746, 698 (characteristic bands due to bptz, PPh$_3$, and counter anion PF$_6^-$); ^{1}H-NMR (δ ppm, CDCl$_3$, 300 MHz, 25 °C): 8.92 (d), 8.78 (d), 8.74 (d), 8.70 (d), 8.11 (t), 8.20 (t), 7.4–7.18 (br, m), 7.02 (t), -12.8 (t, Ru–H); ^{13}C{^{1}H}: δ 204 (carbonyl carbon), 153.89, 150.95, 138.77, 137.85, 128.98, 128.22, 127.08, 126.83 ppm (carbons of the bptz ligand); ^{31}P{^{1}H}: δ 48.6 ppm (s); UV–vis (λ_{max} nm): 399, 394, 241.

3.2.5. Preparation of [RuH(CO)(PPh₃)₂(bppz)PtCl₂]PF₆ (5)

3.2.5. Preparation of [RuH(CO)(PPh$_3$)$_2$(bppz)PtCl$_2$]PF$_6$ (5)

Complex **3** [RuH(CO)(PPh$_3$)$_2$(bppz)]PF$_6$ (517 mg, 0.5 mmol) was dissolved in MeOH (20 ml) and filtered to remove any solid residue. To the filtrate K$_2$PtCl$_4$ (208 mg, 0.5 mmol) was added and the solution was heated under reflux for 24 h. It was cooled to r.t. and filtered. To the red–brown solution thus obtained, a solution of NH$_4$PF$_6$ (163 mg, 1 mmol) dissolved in methanol (10 ml) was added. It was rotaporated to 10 ml and left overnight. A brownish red colored microcrystalline complex appeared. These were filtered, washed with MeOH, Et$_2$O and dried in vacuo. Yield 78%; Anal. Found: C, 54.51; H, 3.77; N, 5.04. Calc. for C$_{51}$H$_{41}$Cl$_2$F$_6$N$_4$OP$_3$PtRu: C, 54.07; H, 3.36; N, 4.75%. FABMS (*m/z*); 1155 (calc for [RuH(CO)(PPh$_3$)$_2$-(bppz)PtCl$_2$]$^+$, 1154); IR (cm^{-1}, nujol): 2006 ν(Ru–H), 1955 ν(CO), 1585, 1575, 1550, 1540, 1520, 1440, 1365, 1312, 1250, 1160, 1035, 986, 845, 735, 690, (bands due to bppz, PPh$_3$ and counter anion PF$_6^-$); ^{1}H-NMR (δ ppm, acetone-d_6, 300 MHz, 25 °C): 9.20 (d), 8.65 (d), 8.16 (m), 8.12–7.80 (m), 7.65–7.52 (m), 7.40–6.94 (br, m), -11.3 (t); ^{31}P{^{1}H}: δ 51.20 ppm (s); UV–vis (λ_{max} nm): 480, 381, 315.

3.2.6. Preparation of [RuH(CO)(PPh₃)₂(bppz)PdCl₂](PF₆) (6)

3.2.6. Preparation of [RuH(CO)(PPh$_3$)$_2$(bppz)PdCl$_2$](PF$_6$) (6)

Complex **6** was prepared by the above procedure starting from [RuH(CO)(PPh$_3$)$_2$(bppz)]PF$_6$ (517 mg, 0.5 mmol) and [PdCl$_2$(benzonitrile)$_2$] (207 mg, 0.5 mmol). It separated as black crystalline product. Yield: 72%; Anal. Found: C, 50.53; H, 3.38; N, 4.62. Calc. for C$_{92}$H$_{76}$F$_6$N$_4$OP$_5$PdRu$_2$: C, 50.03; H, 3.42; N, 4.72%. UV–vis (λ_{max} nm): 472, 352, 315.

3.2.7. Preparation of [RuH(CO)(PPh₃)₂(bppz)(η⁶-C₁₀H₁₄)RuCl](PF₆)₂ (7)

3.2.7. Preparation of [RuH(CO)(PPh$_3$)$_2$(bppz)(η^6-C$_{10}$H$_{14}$)RuCl](PF$_6$)$_2$ (7)

Complex **7** was prepared by reaction of [RuH(CO)-(PPh$_3$)$_2$(bppz)]PF$_6$ (517 mg, 0.5 mmol) in MeOH (20 ml) with [{Ru(η^6-C$_{10}$H$_{14}$)(μ-Cl)Cl}$_2$] following the above procedure. It appeared in the form of a brown–red crystalline solid. Yield: 88%; Anal. Found: C, 48.85; H, 3.91; N, 3.71. Calc. for C$_{61}$H$_{55}$ClF$_{12}$N$_4$OP$_4$Ru$_2$: C, 49.07; H, 3.79; N, 3.86%. FABMS (*m/z*): 1307, (calc. for {[RuH(CO)(PPh$_3$)$_2$(bppz)(η^6-C$_{10}$H$_{14}$)RuCl](PF$_6$)}$^+$ 1304); ^{1}H-NMR (δ ppm, CDCl$_3$, 300 MHz, 25 °C): 9.26 (d), 8.84 (d), 8.48 (m), 8.17–7.88 (m), 7.84–7.36 (m), 7.40–6.92 (br, m), 5.59–5.33 (dd), 2.92 (sep), 2.13 (s) 1.25 (dd), -10.50 (t); ^{31}P{^{1}H}: δ 50.82 ppm (s); UV–vis (λ_{max} nm): 475, 360, 315.

3.2.8. Preparation of [RuH(CO)(PPh₃)₂(bppz)(η⁶-C₆Me₆)RuCl](PF₆)₂ (8)

3.2.8. Preparation of [RuH(CO)(PPh$_3$)$_2$(bppz)(η^6-C$_6$Me$_6$)RuCl](PF$_6$)$_2$ (8)

It was prepared by reaction of [RuH(CO)(PPh$_3$)$_2$-(bppz)]PF$_6$ (517 mg, 0.5 mmol) complex in MeOH (20 ml) with [{Ru(η^6-C$_6$Me$_6$)(μ-Cl)Cl}$_2$]. It separated as dark tan-colored microcrystals. Yield: 70%. Anal. Found: C, 49.76; H, 4.04; N, 3.79. Calc. for C$_{63}$H$_{59}$ClF$_{12}$N$_4$OP$_4$Ru$_2$: C, 50.15; H, 3.99; N, 3.78%. FABMS (*m/z*); 1333, (calc. for {[RuH(CO)(PPh$_3$)$_2$-(bppz)(η^6-C$_6$Me$_6$)RuCl](PF$_6$)}$^+$ 1333); ^{1}H-NMR (δ ppm, CDCl$_3$, 300 MHz, 25 °C), 9.26 (d), 8.84(d), 8.48 (m), 8.17–7.88 (m), 7.84–7.36 (m), 7.40–6.92 (br, m), 5.59–5.33 (dd), 2.92 (sep), 2.13 (s) 1.25 (dd), -10.50 (t); ^{31}P{^{1}H}: δ 50.82 ppm (s); UV–vis (λ_{max} nm): 475, 360, 315.

3.2.9. Preparation of [RuH(CO)(PPh₃)₂(bppz)(η⁵-C₅H₅)(PPh₃)Ru](PF₆)₂ (9)

3.2.9. Preparation of [RuH(CO)(PPh$_3$)$_2$(bppz)(η^5-C$_5$H$_5$)(PPh$_3$)Ru](PF$_6$)$_2$ (9)

Complex **9** was prepared by reaction of [RuH(CO)-(PPh$_3$)$_2$(bppz)]PF$_6$ (517 mg, 0.5 mmol) complex in MeOH (20 ml) with [RuCl(η^5-C$_5$H$_5$)(PPh$_3$)$_2$] (364 mg, 0.5 mmol). It separated as a dark black colored complex. Yield 70%. Anal. Found: C, 55.20; H, 3.82; N, 3.45. Calc. for C$_{74}$H$_{61}$F$_{12}$N$_4$OP$_5$Ru$_2$: C, 55.22; H, 3.79; N, 3.48%. ^{1}H-NMR (δ ppm, DMSO-d_6, 300 MHz, 25 °C): 9.60 (d), 9.17 (d), 8.18 (m), 8.12–7.80 (m), 7.88–6.94 (br, m), 5.4 (sharp s, Cp), -11.9 (t); UV–vis. (λ_{max} nm): 544, 362, 315.

3.2.10. Preparation of [RuH(CO)(PPh₃)₂(bppz)Rh(η⁵-C₅Me₅)Cl](PF₆)₂ (10)

3.2.10. Preparation of [RuH(CO)(PPh$_3$)$_2$(bppz)Rh(η^5-C$_5$Me$_5$)Cl](PF$_6$)$_2$ (10)

Complex **10** was prepared following the above procedure from [RuH(CO)(PPh$_3$)$_2$(bppz)]PF$_6$ (517 mg, 0.5 mmol) and [{(η^5-C$_5$Me$_5$)RhCl$_2$}$_2$] (314 mg, 0.5 mmol). It separated as a red microcrystalline solid. Yield: 75%; Anal. Found: C, 49.72; H, 3.88; N, 3.87. Calc. for C$_{61}$H$_{56}$ClF$_{12}$N$_4$OP$_4$RhRu: C, 50.41; H, 3.85; N, 3.85%. FABMS (*m/z*): 1309, (calc. for {[RuH(CO)(PPh$_3$)$_2$-(bppz)Rh(η^5-C$_5$Me$_5$)Cl](PF$_6$)}$^+$, 1307); ^{1}H-NMR (δ ppm, DMSO-d_6, 300 MHz, 25 °C): 9.16 (d), 8.82 (d),

8.45 (m), 8.13–7.81 (m), 7.84–7.36 (m), 7.36–6.94 (br, m), 1.60(s, C_5Me_5) − 11.2 (t); $^{31}P\{^1H\}$: δ 50.62 ppm (s); UV–vis (λ_{max} nm): 465, 360, 315.

3.3. X-ray structure determination of [RuH(CO)(PPh$_3$)$_2$(tptz)]BF$_4$

A crystal suitable for X-ray diffraction analysis was mounted onto a glass fiber and transferred to an AFC6S-Rigaku automatic diffractometer ($T = 290$ K, Mo–K$_\alpha$ radiation, graphite monochromator, $\lambda = 0.71073$ Å). Accurate unit cell parameters and an orientation matrix were determined by least-squares fitting from the settings of 25 high-angle reflections. Crystal data and details on data collection and refinements are given in Table 1. Data were collected by the $\omega/2\theta$ scan method. Lorentz and polarization corrections were applied. Decay and semi-empirical absorption correction (ψ method) were also applied. Patterson methods and subsequent expansion of the models using DIRDIF [19] solved the structure. Reflections having $I > 3\sigma(I)$ were used for structure refinement. Ru, N and C atoms of the N, N′–$C_{15}H_{12}N_6$ ligand were anisotropically refined and the remaining non-hydrogen atoms were isotropically refined. The H(1) was localized in a regular difference Fourier map and the remaining hydrogen atoms included at idealized positions. The hydrogen atoms were not refined. All calculations for data reduction, structure solution, and refinement were carried out on a VAX 3520 computer at the Servicio Central de Ciencia y Technologia de la Universidad de Cadiz, using the TEXSAN [20] software system and ORTEP [21] for plotting. Maximum and minimum peaks in the final difference Fourier mass were $+1.26$ and -1.16 e Å^{-3}.

4. Supplementary material

Crystallographic data for the structural analysis in CIF format have been deposited with the Cambridge Crystallographic Data Centre, CCDC no. 140169 for the complex [RuH(CO)(PPh$_3$)$_2$(tptz)]BF$_4$. Copies of this information may be obtained free of charge from The Director, CCDC, 12 Union Road, Cambridge CB2 1EZ, UK (Fax: $+44$-1223-336033; e-mail: deposit@ccdc.cam.ac.uk or www: http://www.ccdc.cam.ac.uk).

References

[1] (a) K. Kalyansundaram, Photochemistry of Polypyridine and Porphyrin Complexes, Academic Press, London, 1991;
(b) V. Balzani, F. Scandola, Supramolecular Photochemistry, Horwood, Chichester, UK, 1991;
(c) J.-M. Lehn, Supramolecular Chemistry, VCH, Weinheim, 1995;
(d) V. Balzani, A. Juris, M. Venturi, S. Campagna, S. Serroni, Chem. Rev. 96 (1996) 96;
(e) A. Kirsch-De Mesmaeker, G.P. Leconte, G.M. Kelly, Top. Curr. Chem. 177 (1996) 25;
(f) L. De Cola, P. Belser, Coord. Chem. Rev. 117 (1998) 301;
(g) F. Bargiletti, L. Flamigni, Chem. Soc. Rev. 29 (2000) 1.
[2] (a) R.E. Dessy, J.C. Charkoundian, T.P. Abeles, A.L. Rheingold, J. Am. Chem. Soc. 92 (1970) 3947;
(b) C. Cruetz, N. Sutin, B.S. Brunschwis, J. Am. Chem. Soc. 101 (1979) 1297;
(c) G.M. Brown, B.S. Brunschwis, C. Creutz, J.N. Endicoff, N. Sutin, J. Am. Chem. Soc. 101 (1979) 1298.
[3] (a) N. Gupta, N. Grover, G.A. Neyhart, P. Singh, H.H. Thorp, Inorg. Chem. 32 (1993) 310;
(b) E. Brauns, W. Sumner, J.A. Clark, S.M. Molnar, Y. Kawanishi, K.J. Brewer, Inorg. Chem. 36 (1997) 2861;
(c) J.-D. Lee, L.M. Vrana, E.R. Bullock, K.J. Brewer, Inorg. Chem. 37 (1998) 3575;
(d) C. Ceroni, F. Paolucci, S. Roffia, S. Serroni, S. Campagna, A.J. Bard, Inorg. Chem. 37 (1998) 2829;
(e) A. Klein, V. Kasack, R. Reinhardt, S. Torsten, T. Scheiring, S. Zalis, J. Fiedler, W. Kaim, J. Chem. Soc. Dalton Trans. 0 (1999) 575;
(f) P. Paul, B. Tyagi, A.K. Bilakhia, D. Parthsarthi, E. Suresh, Inorg. Chem. 39 (2000) 14;
(g) G. Albano, P. Belser, C. Dual, Inorg. Chem. 40 (2001) 1408.
[4] D.S. Pandey, A.N. Sahay, M.G. Walwalkar, J. Organomet. Chem. 613 (2000) 250 and references therein.
[5] (a) B. Hasenknopf, J.-M. Lehn, N. Boumediene, G.A. Dupont, A. Van Dorsselaer, B. Kneisel, D. Fenske, J. Am. Chem. Soc. 119 (1997) 10956;
(b) E. Ishow, A. Gourdon, J.-P. Launay, C. Chiroboli, F. Scandola, Inorg. Chem. 38 (1999) 1504.
[6] (a) R.P. Thummel, Y. Jahng, Inorg. Chem. 25 (1986) 2527;
(b) G.S. Hanan, C.R. Arana, J.-M. Lehn, G. Baum, D. Fenske, Chem. Eur. J. 2 (1996) 1292.
[7] D.K. Gupta, O.S. Sisodia, A.N. Sahay, D.S. Pandey, Synth. React. Inorg. Metal-Org. Chem. 28 (1998) 355.
[8] P. Didier, I. Ortmans, A. Kirsch- De Mesmaeker, R.J. Watts, Inorg. Chem. 34 (1993) 5239.
[9] R.M. Berger, D.D. Elis II, Inorg. Chim. Acta 241 (1996) 1.
[10] B.P. Sullivan, D.J. Salmon, T.J. Meyer, Inorg. Chem. 17 (1978) 3334.
[11] R. Rillema, K.B. Mack, Inorg. Chem. 21 (1982) 3849.
[12] (a) L. Vogler, B. Scott, K.J. Brewer, Inorg. Chem. 36 (1993) 898;
(b) S.M. Molnar, K.R. Nevile, G.E. Gensen, K.J. Brewer, Inorg. Chim. Acta 206 (1993) 69;
(c) S.D. Earnst, W. Kaim, Inorg. Chem. 28 (1989) 1520.

[13] (a) H. Ishida, K. Tanaka, T. Tanaka, Chem. Lett. (1995) 405;
(b) H. Ishida, K. Tanaka, T. Tanaka, Organometallics 6 (1987) 181;
(c) C.M. Bollinger, B.P. Sullivan, D. Conrad, J.A. Gilbert, N. Storg, T.J. Meyer, J. Chem. Soc. Chem. Commun. (1985) 796.

[14] P. Ghosh, A. Chakravorty, Inorg. Chem. 36 (1997) 64 and references therein.

[15] (a) M.F. McGuiggan, L.H. Pignolet, Inorg. Chem. 21 (1982) 2523;
(b) A. Sahajpal, S.D. Robinson, M.A. Mazid, M. Motevalli, M.B. Hursthouse, J. Chem. Soc. Dalton Trans. (1990) 2119.

[16] (a) G.J. Philip, J.R. Steven, C.-L- Lee, B.R. Jamer, Inorg. Chem. 30 (1991) 4617;
(b) R. Atencio, B. Christina, M.A. Esteruelas, J.L. Fernando, L.A. Oro, J. Chem. Soc. Dalton Trans. (1995) 2171;
(c) M.R. Churchill, K.M. Keil, F.V. Bright, S. Pandey, G.A. Baker, J.B. Keister, Inorg. Chem. 39 (2000) 5807.

[17] A. Cantarero, J.M. Amigo, J. Faus, M. Julve, T. Debaerdemaeker, J. Chem. Soc. Dalton Trans. (1988) 2033.

[18] N. Ahmad, J.J. Levison, S.D. Robinson, M.F. Uttley, Inorg. Synth. 15 (1974) 45.

[19] P.T. Beursken, DIRDIF, Technical Report 1984/1, Crystallography Laboratory Toernooiveld, 1984.

[20] TEXSAN, Single-Crystal Structure Analysis Software, Version 5.0, Molecular Structure Corporation, Houston Texas, TX, 1989.

[21] C.K. Johnson, ORTEP, A Thermal Ellipsoid Plotting Program, Oak Ridge National Laboratory, Oak Ridge, TN, 1965.